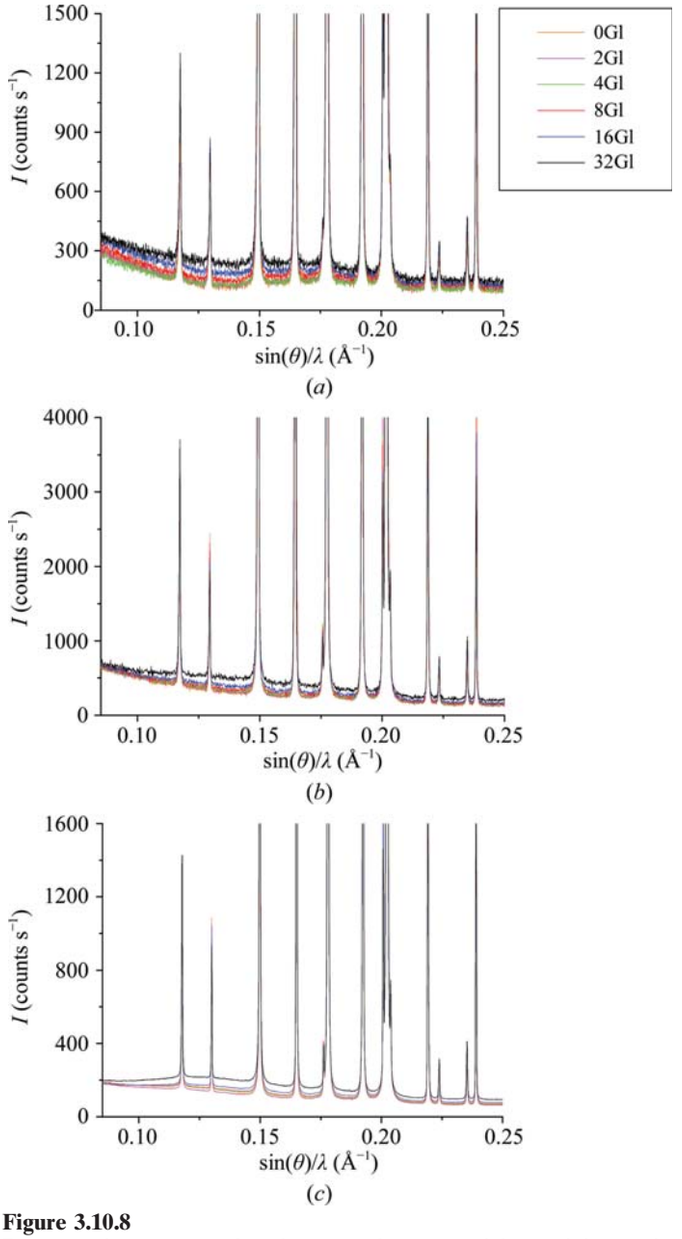

Figure 3.10.8
Raw powder patterns for the amorphous-material-containing series composed of a constant matrix of calcite and zincite, and increasing amounts of ground glass. Quartz was added as internal standard. (*a*) Mo $K\alpha_1$, (*b*) Cu $K\alpha_1$ and (*c*) SXRPD radiations. The intensities of the patterns have been rescaled to highlight the contributions of the glass to the background.

be pointed out that for the Mo $K\alpha_1$ analyses the value from the measurement of the Gl-free sample, 3.5 wt%, matches the value from the *y* intercept of the plot, 3.7 wt%, very well. Meanwhile, there is a much larger discrepancy for the similar Cu-based analyses, 12.0 and 10.0 wt%, respectively, which is quite far from zero. Hence, it is concluded that the amorphous contents derived from Mo $K\alpha_1$ data are more accurate than those derived from Cu $K\alpha_1$ data. However, it is not possible to reliably quantify amorphous contents below ∼8–10 wt% from Mo $K\alpha_1$ and Cu $K\alpha_1$ diffraction data (see Table 3.10.4) with the internal-standard method.

On the contrary, SXRPD reliably allows quantification of amorphous contents down to ∼2 wt% for this relatively simple mixture. In addition, the AKLD and the KLD values reported in Table 3.10.4 demonstrate that the synchrotron analyses are indeed much better than the laboratory analyses.

3.10.10. Conclusions

(i) We have thoroughly studied the limit of detection for a well crystallized inorganic phase in an inorganic compound matrix. We have determined the following LoDs for insoluble anhydrite: ∼0.2 wt%, ∼0.3 wt% and lower than 0.1 wt% for Cu $K\alpha_1$, Mo $K\alpha_1$ and synchrotron radiations, respectively. We conclude that the LoD is slightly better for Cu $K\alpha_1$ than for Mo $K\alpha_1$ because the λ^3 dependence of the diffraction intensity, with similar acquisition times, yielded slightly better signal-to-noise ratios in the Cu patterns. Of course, detector efficiencies also play a role in the measured signal-to-noise ratios.

(ii) We have also studied the limit of quantification for a well crystallized inorganic phase using laboratory X-ray powder diffraction. This phase could be quantified at the level of 0.12 wt% in stable fits with repeatable outputs and good precision. However, the accuracy of these analyses was quite poor, with relative errors close to 100%. Only contents higher than 1.0 wt% yielded analyses with relative errors lower than 20%.

(iii) The Rietveld quantitative phase analysis results from high-resolution Mo $K\alpha_1$ powder diffraction (transmission geometry) and high-resolution Cu $K\alpha_1$ powder diffraction (reflection geometry) were quite similar for a series of crystalline inorganic phase samples. We inferred the validation of the Mo-based analyses procedure from this initial study, as it yielded results very close to well established high-resolution Cu radiation analyses (see Fig. 3.10.7*a*). From the comparison of the AKLD values for the two types of analyses, it was demonstrated that the Mo $K\alpha_1$ analyses were slightly better than those using Cu $K\alpha_1$.

(iv) Comparison of the results obtained from Mo-based and Cu-based patterns for a series of crystalline organic phase mixtures showed that the Mo $K\alpha_1$ analyses gave slightly more accurate values. This conclusion was drawn because the calibration curve obtained from Mo patterns with increasing content of xylose gave an R^2 value closer to 1.0, a slope closer to 1.0 and an intercept value close to 0.0 (see Fig. 3.10.7*b*). The slightly poorer results from Cu $K\alpha_1$ analyses are very likely to be due to the transparency effects in reflection geometry.

(v) Comparison of the results obtained from Mo $K\alpha_1$ and Cu $K\alpha_1$ patterns for a series containing increasing amounts of amorphous glass also indicated that the Mo-based analyses were slightly more accurate than the corresponding Cu $K\alpha_1$ analyses. This conclusion was drawn because the obtained calibration curve from the Mo data has (1) a slope closer to 1.0, (2) a smaller amorphous value for the glass-free sample and (3) a closer agreement between the intercept from the least-squares fit and the determined amorphous value for the glass-free sample (see Fig. 3.10.7*c*). The AKLD analysis confirmed this outcome. Furthermore, the results from synchrotron data have the best accuracy, as shown by the calibration plot and the AKLD analysis.

Finally, we conclude that for the challenging quantification analyses studied here, the results derived from high-energy Mo $K\alpha_1$ patterns were slightly more accurate than those obtained from Cu $K\alpha_1$ patterns. We justify this conclusion based on the larger tested volume for Mo $K\alpha_1$ analyses, which led to better statistics/accuracy in the recorded powder-pattern intensities. The minimization of microabsorption in the Mo $K\alpha_1$ transmission

data is very likely to be an additional factor in the improved accuracy.

This chapter is based on an article *Accuracy in Rietveld quantitative phase analysis: a comparative study of strictly monochromatic Mo and Cu radiations* by León-Reina *et al.* [(2016), *J. Appl. Cryst.* **49**, 722–735]. The work was supported by Spanish MINECO through BIA2014-57658-C2-2-R, which is co-funded by FEDER, and BIA2014-57658-C2-1-R research grants. Funding from Junta de Andalucía (grant P11-FQM-07517) is also acknowledged. We thank CELLS-ALBA (Barcelona, Spain) for providing synchrotron beam time on the BL04-MSPD beamline. All raw powder-diffraction data files underlying this work can be accessed at Zenodo at https://doi.org/10.5281/zenodo.1291900 and used under the Creative Commons Attribution license.

References

Albertsson, J., Abrahams, S. C. & Kvick, Å. (1989). *Atomic displacement, anharmonic thermal vibration, expansivity and pyroelectric coefficient thermal dependences in ZnO. Acta Cryst.* B**45**, 34–40.

Aranda, M. A. G., De la Torre, Á. G. & León-Reina, L. (2012). *Rietveld quantitative phase analysis of OPC clinkers, cements and hydration products. Rev. Mineral. Geochem.* **74**, 169–209.

Bezou, C., Nonat, A., Mutin, J.-C., Christensen, A. N. & Lehmann, M. S. (1995). *Investigation of the crystal structure of γ-$CaSO_4$, $CaSO_4$·0.5H_2O, and $CaSO_4$·0.6H_2O by powder diffraction methods. J. Solid State Chem.* **117**, 165–176.

Brown, G. M. & Levy, H. A. (1979). *α-D-Glucose: further refinement based on neutron-diffraction data. Acta Cryst.* B**35**, 656–659.

Buhrke, V. E., Jenkins, R. & Smith, D. K. (1998). *A Practical Guide for the Preparation of Specimens for X-ray Fluorescence and X-ray Diffraction Analysis.* New York: Wiley.

Cuesta, A., Álvarez-Pinazo, G., García-Maté, M., Santacruz, I., Aranda, M. A. G., De la Torre, Á. G. & León-Reina, L. (2015). *Rietveld quantitative phase analysis with molybdenum radiation. Powder Diffr.* **30**, 25–35.

De La Torre, A. G., Bruque, S. & Aranda, M. A. G. (2001). *Rietveld quantitative amorphous content analysis. J. Appl. Cryst.* **34**, 196–202.

De la Torre, Á. G., López-Olmo, M., Álvarez-Rua, C., García-Granda, S. & Aranda, M. A. G. (2004). *Structure and microstructure of gypsum and its relevance to Rietveld quantitative phase analyses. Powder Diffr.* **19**, 240–246.

Dollase, W. A. (1986). *Correction of intensities for preferred orientation in powder diffractometry: application of the March model. J. Appl. Cryst.* **19**, 267–272.

Egami, T. & Billinge, S. J. L. (2003). *Underneath the Bragg Peaks. Structural Analysis of Complex Materials.* Amsterdam: Pergamon.

Elton, N. J. & Salt, P. D. (1996). *Particle statistics in quantitative X-ray diffractometry. Powder Diffr.* **11**, 218–229.

Fauth, F., Peral, I., Popescu, C. & Knapp, M. (2013). *The new material science powder diffraction beamline at ALBA synchrotron. Powder Diffr.* **28**, S360–S370.

Fries, D. C., Rao, S. T. & Sundaralingam, M. (1971). *Structural chemistry of carbohydrates. III. Crystal and molecular structure of 4-O-β-D-galactopyranosyl-α-D-glucopyranose monohydrate (α-lactose monohydrate). Acta Cryst.* B**27**, 994–1005.

García-Maté, M., Santacruz, I., Cuesta, A., León-Reina, L., Aranda, M. A. G., Baco, I., Morin, V., Walenta, G., Gartner, E. & De la Torre, A. G. (2014). *Amorphous content determination in calcium sulfoaluminate related materials by external and internal standard methodologies. Adv. Cem. Res.* **27**, 417–423.

Garske, D. & Peacor, D. R. (1965). *Refinement of the structure of celestite $SrSO_4$. Z. Kristallogr.* **121**, 204–210.

Hordvik, A. (1971). *The crystal and molecular structure of α-xylose. Acta Chem. Scand.* **25**, 2175–2182.

Kanters, J. A., Roelofsen, G., Alblas, B. P. & Meinders, I. (1977). *The crystal and molecular structure of β-D-fructose, with emphasis on anomeric effect and hydrogen-bond interactions. Acta Cryst.* B**33**, 665–672.

Kirfel, A. & Will, G. (1980). *Charge density in anhydrite, $CaSO_4$, from X-ray and neutron diffraction measurements. Acta Cryst.* B**36**, 2881–2890.

Kullback, S. (1968). *Information Theory and Statistics*, pp. 1–11. New York: Dover.

Larson, A. C. & Von Dreele, R. B. (2000). *General Structure Analysis System (GSAS)*. Los Alamos National Laboratory Report LAUR 86-748.

León-Reina, L., De la Torre, A. G., Porras-Vázquez, J. M., Cruz, M., Ordonez, L. M., Alcobé, X., Gispert-Guirado, F., Larrañaga-Varga, A., Paul, M., Fuellmann, T., Schmidt, R. & Aranda, M. A. G. (2009). *Round robin on Rietveld quantitative phase analysis of Portland cements. J. Appl. Cryst.* **42**, 906–916.

León-Reina, L., García-Maté, M., Álvarez-Pinazo, G., Santacruz, I., Vallcorba, O., De la Torre, A. G. & Aranda, M. A. G. (2016). *Accuracy in Rietveld quantitative phase analysis: a comparative study of strictly monochromatic Mo and Cu radiations. J. Appl. Cryst.* **49**, 722–735.

Madsen, I. C., Scarlett, N. V. Y., Cranswick, L. M. D. & Lwin, T. (2001). *Outcomes of the International Union of Crystallography Commission on Powder Diffraction Round Robin on Quantitative Phase Analysis: samples 1a to 1h. J. Appl. Cryst.* **34**, 409–426.

Madsen, I. C., Scarlett, N. V. Y. & Kern, A. (2011). *Description and survey of methodologies for the determination of amorphous content via X-ray powder diffraction. Z. Kristallogr.* **226**, 944–955.

Maslen, E. N., Streltsov, V. A., Streltsova, N. R. & Ishizawa, N. (1995). *Electron density and optical anisotropy in rhombohedral carbonates. III. Synchrotron X-ray studies of $CaCO_3$, $MgCO_3$ and $MnCO_3$. Acta Cryst.* B**51**, 929–939.

Scarlett, N. V. Y., Madsen, I. C., Cranswick, L. M. D., Lwin, T., Groleau, E., Stephenson, G., Aylmore, M. & Agron-Olshina, N. (2002). *Outcomes of the International Union of Crystallography Commission on Powder Diffraction Round Robin on Quantitative Phase Analysis: samples 2, 3, 4, synthetic bauxite, natural granodiorite and pharmaceuticals. J. Appl. Cryst.* **35**, 383–400.

Stutzman, P. (2005). *Powder diffraction analysis of hydraulic cements: ASTM Rietveld round-robin results on precision. Powder Diffr.* **20**, 97–100.

Thompson, P., Cox, D. E. & Hastings, J. B. (1987). *Rietveld refinement of Debye–Scherrer synchrotron X-ray data from Al_2O_3. J. Appl. Cryst.* **20**, 79–83.

Von Dreele, R. B. & Rodriguez-Carvajal, J. (2008). *Powder Diffraction: Theory and Practice*, edited by R. E. Dinnebier & S. J. L. Billinge, pp. 58–88. Cambridge: Royal Society of Chemistry. https://doi.org/10.1039/9781847558237-00058.

Will, G., Bellotto, M., Parrish, W. & Hart, M. (1988). *Crystal structures of quartz and magnesium germanate by profile analysis of synchrotron-radiation high-resolution powder data. J. Appl. Cryst.* **21**, 182–191.

Zevin, L. S. & Kimmel, G. (1995). *Quantitative X-ray Diffractometry*. New York: Springer-Verlag.